Agricultural and Forest Meteorology
Volume 297, 15 February 2021, 108240

Spatial-temporal dynamics of maize and soybean planted area, harvested area, gross primary production, and grain production in the Contiguous United States during 2008-2018

Xiaocui Wu [a], Xiangming Xiao [a] ✉, Zhengwei Yang [b], Jie Wang [a], Jean Steiner [c], Rajen Bajgain [a]

https://doi.org/10.1016/j.agrformet.2020.108240

Highlight

- Planted area derived from CDL maps is highly consistent with NASS area statistic data
- Annual GPP_{VPM} had strong linear relationships with maize and soybean grain production.
- The Harvest Index calculated from grain production and GPP_{VPM} have small interannual variation.
- The cumulative GPP_{VPM} accounted for ~90% of variance in grain production by the end of July.

Abstract

The United States of America ranked first in maize export and second in soybean export in the world. Accurate and timely data and information on maize and soybean production in the Contiguous United States (CONUS) are important for food security at the regional and global scales. In this study, we firstly compare the maize and soybean planted area from cropland data layer (CDL) with NASS area statistics over the CONUS during 2008-2018, and evaluate the interannual changes of planted and harvested area based on the two datasets. Secondly, we investigate the relationship between grain production and gross primary production (GPP) simulated by Vegetation Photosynthesis Model (VPM) at national and county scales. Finally, we evaluate the linear regression models between grain production and cumulated GPP_{VPM} over time at 8-day resolution. We found strong spatial-temporal consistency between CDL and NASS datasets in maize and soybean planted areas. Maize and soybean planted areas increased by mid-2010s, largely driven by markets and international trade. Severe summer drought in 2012 had little impact on soybean planted and harvested area and maize planted area, but substantially reduced maize harvested area, and grain

production. Annual county-level GPP_{VPM} had strong linear relationship with NASS grain production for maize and soybean. The Harvest Index, defined as the ratio between grain production and GPP_{VPM} (HI_{GPP_VPM}), ranged from 0.25 (2012) to 0.36 for maize and from 0.13 to 0.15 for soybean. The linear regression models between grain production and cumulated GPP_{VPM} (GPP_{VPM_CUM}) over time at 8-day resolution showed that by the end of July, GPP_{VPM_CUM} accounted for ~90% of variance in maize and soybean grain production, which was approximately two months before farmers started to harvest. This study clearly shows that VPM and GPP_{VPM} data are useful for monitoring and in-season forecasting of maize and soybean grain production in the CONUS.

Previous Next

Keywords

Crop production; Gross primary production; Vegetation Photosynthesis Model; Planted area; Harvest Index; in-season forecasting

1. Introduction

Crop production and food security is one of fundamental challenges in our society due to the rising global population, dietary change, climate change, and increasing biofuel production that uses crops as feedstock (Ray et al. 2013). Maize (Zea maize, L) and soybean (Glycine max) are two of the major sources of caloric energy for human and are critical for world food supply. The United States of America (USA) is the largest maize and soybean producer in the world (Meade et al. 2016) and ranked first in maize export and second in soybean export in the world. Inter-annual change of maize and soybean area and grain production in the USA affect the world grain trade market (Gardiner 2016). Therefore, accurate and timely information and knowledge on planted area, harvested area, grain production and grain yield of maize and soybean in the USA is crucial for agriculture, food security, and international trade (Iizumi and Ramankutty 2015; Tilman et al. 2011).

Crop grain production, the amount of grains from crop produced in one calendar year in an area of interest (e.g., farm, county, state, country), is the product of crop harvested area and crop grain yield. For crop production estimation, it is essential to have the information of both harvested area and grain yield. The National Agricultural Statistics Service (NASS) of the United States Department of Agriculture (USDA) provide annual crop reports for planted area, harvested area, grain yield, and grain production in a year at various administration levels (e.g., national, state and county). The data collection through sample-based agricultural surveys is not only time consuming and costly but also have long time lags and data gaps (Doraiswamy et al. 2003).

Satellite-based remote sensing has been used to monitor cropping area, grain yield, and grain production since the early 1970s (Atzberger 2013; Fritz et al. 2019; Lobell 2013). Notable progress has been made in satellite-based mapping of cropland areas (planted area and/or harvested areas) at various spatial scales (Cai et al. 2018; Massey et al. 2017; Wang et al. 2019; Wardlow and Egbert 2008; Zhong et al. 2014). A number of studies reported annual maps of maize and soybean area for a few states or counties in the corn-belt region (Cai et al. 2018; Wang et al. 2019; Wardlow and Egbert 2008; Zhong et al. 2014), using 30-m Landsat data (Cai et al. 2018; Wang et al. 2019; Zhong et al. 2014), 500-m MODIS data (Massey et al. 2017; Wardlow and Egbert 2008) and/or 10-m Sentinel-2 data (Belgiu and Csillik 2018). One study generated annual maps of croplands over the contiguous United States (CONUS) with MODIS images at 250-m spatial resolution during 2001-2014 (Massey et al. 2017). The overall accuracy of those crop maps ranged from 60 to 96% (Cai et al. 2018; Massey et al. 2017; Wang et al. 2019; Wardlow and Egbert 2008; Zhong et al. 2014). The USDA-NASS also generated the Cropland Data Layer (CDL) product (Boryan et al. 2011), which includes all major crop types in CONUS. The CDL dataset that covers all the states in CONUS at 30-m spatial resolution started in 2008, and it is widely used in the studies of crop yield in various states or region (Guan et al. 2016; He et al. 2018; Marshall et al. 2018). However, only a few studies have reported the accuracy of CDL-derived planted area in a specific year (Boryan et al. 2011) or in a few states (He et al. 2018). There is a need to investigate the spatial-temporal consistency between CDL-derived planted area and NASS area statistics and to better understand the spatial-temporal dynamics of maize and soybean planted area, harvested area over the entire CONUS during 2008-2018 based on the two datasets..

Grain yield (metric ton/ha) and grain production (metric ton) of maize and soybean crops are a function of aboveground biomass (AGB), gross and net primary production (GPP, NPP), which can be estimated by satellite images and models (Guan et al. 2016; He et al. 2018; Marshall et al. 2018; Sakamoto et al. 2014; Xin et al. 2013). Harvest Index (HI) is calculated as the ratio between crop grain yield and crop aboveground biomass (HI_{AGB}), or NPP (HI_{NPP}) or GPP (HI_{GPP}). Several studies evaluated the relationship between vegetation indices and grain yields of maize and soybean at county scale from the NASS crop statistics (Becker-Reshef et al. 2010; Burke and Lobell 2017; Johnson 2016). Some studies used vegetation indices to estimate crop aboveground biomass and used the AGB-based harvest index (HI_{AGB}) to estimate grain yield, and the resultant yield estimates were compared with the yield data from the NASS crop statistics at county scale (Guan et al. 2016; Lobell et al. 2002). GPP can be estimated by using a light use efficiency (LUE) model driven by remote sensing images and climate data, and the regional and global GPP data products are available to the public (Running et al. 2004; Wu et al. 2018; Zhang et al. 2017). Some studies used the model-based GPP to estimate NPP, AGB and grain yield, and then compared the resultant yield estimates with the yield data from the NASS crop statistics at the county scale, for example, croplands in the Midwest during 2009-2012 (Xin et al. 2013), and croplands in the CONUS during 2010-2015 (Marshall et al. 2018). These studies reported moderate relationships between the model-based yield estimates and the yield data from NASS crop statistics, with a range of R^2 values from 0.5 to 0.7. The resultant moderate relationships in these studies may be explained in part by large variation of the AGB-based harvest index (HI_{AGB}) among crop types and environment (Hay 1995; Lobell et al. 2002) and by the sampling approach in the NASS crop statistics. The NASS crop yield data in a county are based on the sample crop fields in a county, thus the number and spatial distribution of these sample crop fields would affect the yield estimates. Recently, one study used model-based GPP and harvest index (HI_{GPP}) to estimate grain yields of several crops and compare them with the yield/production data from the NASS statistics reports for Montana during 2008-2015 (He et al. 2018). There is a need to evaluate the relationship between GPP and grain production at county and state scales in CONUS during 2008-2018, and how this relationship will change over the crop growing season to facilitate in-season grain production estimation.

In this study we addressed the above-mentioned three research needs on maize and soybean croplands in the CONUS. Our first objective is to evaluate the consistency between CDL-derived planted area and NASS area statistic data and to quantify the spatial-temporal dynamics of maize and soybean planted area and harvested area in the CONUS during 2008-2018. We analyzed the agricultural statistical data of maize and soybean (planted area, harvested area) from the USDA NASS and satellite-based planted area of maize and soybean from the USDA Cropland Data Layer (CDL) dataset during 2008-2018. Our second objective is to better understand the relationships between GPP and grain production at county scale during 2008-2018. We analyzed the GPP data from the satellite-based Vegetation Photosynthesis Model (VPM) (Wu et al. 2018) and MOD17 algorithm (Running et al. 2004), and grain production data from the NASS. The analysis will quantify the relationships between maize and soybean GPP and grain production from NASS crop statistics at county and national scale under varying climate conditions (drought year versus normal years). During the period of 2008-2018, severe drought and heatwave events occurred in various regions of CONUS, for example, the 2012 summer drought, which was reported as one of the worst droughts since 1988. Our third objective is to explore the potential of using cumulated GPP over time to estimate grain production in a year. We calculated cumulated GPP_{VPM} over the maize and soybean growing season and analyze the relationship between cumulated GPP_{VPM} and grain production of maize and soybean in CONUS at county scale. The analysis will develop a simple linear regression model that can do in-season forecasting (early prediction) of grain production of maize and soybean croplands in CONUS before farmers start to harvest maize and soybean crops.

2. Materials and methods

2.1. Study area

The study area is the contiguous United States (CONUS). It covers 48 states and 3,233 counties. Climate in the CONUS ranges from subtropical climate in the southern region (e.g., Florida) to temperate climate in the northern region. Crop cultivation is dominated by a single crop per year, and major crop types include maize (~35%), soybean (~33%), winter wheat (~22%), and sorghum (~3%). There are noticeable geographical patterns of major crop types in CONUS, for example, the Great Plains region is dominated with wheat, maize, soybean, and the regions around the Great Lakes are dominated with maize and soybean, known as the Corn-Belt.

2.2. USDA-NASS statistical data – crop planted area, harvested area, and grain production during 2008-2018

The annual county and national statistics data of crop planted area (acre), harvested area (acre), grain production (bushel) and grain yield (bushel/acre) for maize and soybean from 2008 to 2018 were downloaded from the USDA-NASS Quick Stats Database (https://quickstats.nass.usda.gov/). For summer crops, the NASS planted and harvested area were mostly based on the June Agricultural Survey (JAS) data. During the first two weeks of June, producers in the designated sample farms are asked by investigators about the acreage and other information by crop, including planted and/or intend-to-plant areas, and the acreage they intend to harvest (USDA, 2018). The yield statistics were based on two large panel surveys that are annually conducted throughout the growing season. One is the Agricultural Yield Survey (AYS), which is based on farmers' reported yield information for most crops. Each year, a subsample of farmers who responded to the list portion of the JAS, are contacted monthly by phone during the growing season (August to November) and asked to provide expected crop yield. The other is the Objective Yield Survey (OYS), which provides independent yield estimates by aggregating field biophysical crop measurements into a model (USDA, 2018). These biophysical crop measurements, such as plant counts per unit area, grain size, were sampled in the fields across the major crop growing areas. The OYS is very costly and is conducted only in the top crop production states. Ultimately, the results from both the AYS and OYS surveys are analyzed by the NASS Agricultural Statistics Board (ASB) to establish the yield estimates. The NASS crop grain production (bushel) is estimated from the expected harvested area and grain yield at the survey date and predicted assuming normal conditions for the remainder of the crop growing season. For grain production of maize and soybean, we converted bushel to metric ton by using the conversion factors of 0.0254 ton/bu (maize) and 0.0272 ton/bu (soybean), respectively (Guan et al. 2016).

2.3. USDA-NASS Cropland Data Layers (CDL) – crop planted area during 2008-2018

The annual CDL dataset at 30-m spatial resolution is a remote sensing-based land cover product. The CDL product utilizes both in-situ ground reference data and multiple satellite imagery to identify and map field crops. The major sources of agricultural and non-agricultural ground reference data, which were used as training data in the supervised classification, includes the USDA's Farm Service Agency (FSA) Common Land Unit (CLU) data and the National Land Cover Database 2001 (NLCD2001). The CLU-based data were collected in every growing season when producers reported crop types and crop acreage in their fields to the FSA county offices. The major remote sensing images used by the CDL classifier include AWiFS, Landsat TM and ETM+, Deimos-1 and UK-DMC-2 and MODIS satellite data. Before 2009, the 56-m AWiFS data was the primary source of imagery and the 30-m Landsat data were used as supplementary source because AWiFS has a higher temporal resolution of 5-day than Landsat (16-day), which provides the opportunity for having more cloud-free observations throughout the crop growing season. The resultant CDL data in 2008-2009 had a spatial resolution of 56-m. During the growing season of 2009, some technical issues happened in AWiFS and the increased competition from international customers disrupted the continuing use of AWiFS data. As a result, Landsat became a primary source of images after 2009 (Boryan et al. 2011). The CDL data in 2010-2018 has a spatial resolution of 30 meter. In 2018, the CDL data from 2008-2009 were reproduced to 30 meters to match the spatial resolution since 2010. In this study, we used the 30-m CDL data throughout 2008-2018 to keep our analysis in a consistent spatial resolution.

The CDL dataset includes more than 100 crop types, with classification accuracy higher than 90% for major crops (maize, soybean and winter wheat) (Boryan et al. 2011). It has been widely used in applications related to land use and land cover change, agricultural sustainability, and agricultural production decision-making. To make use of the dataset more effective and efficient, CropScape, an interactive Web-based CDL data portal, was developed to visualize, query, and analyze CDL data through standard geospatial web services in a publicly accessible online environment (Han et al. 2012). In this study, the CropScape was used to calculate the annual planted areas of maize and soybean at the county scale during 2008-2018. The planted area of maize (soybean) in each county is a sum of all the pixels which are classified as maize (soybean) within the county. The annual planted areas of maize and soybean at the national scales were calculated by adding the areas of all the counties in the nation for each year.

2.4. The input datasets for regional simulation of the Vegetation Photosynthesis Model

The input datasets for simulations of the VPM model include climate (air temperature and radiation), vegetation indices (VIs), and land cover data. The NCEP climate dataset was used for simulations of VPM at the global scale (Zhang et al. 2017) and the NCEP/NARR climate dataset was used for regional simulation of VPM in the North America and the CONUS (Wu et al. 2018; Zhang et al. 2016). In this study, we continued to use the NCEP/NARR data for VPM simulation in the CONUS. The original 3-hourly NARR data with a spatial resolution of 32 km were first aggregated into daily maximum/minimum/mean air temperature, daily daytime mean air temperature, and daily shortwave radiation. The resultant daily data were fi

aggregated to 8-day intervals to match the MODIS data by calculating the averages for air temperature and the sum for downward shortwave radiation in each 8-day period. The 8-day climate data with a coarse resolution of 32 km were then interpolated to 500-m by applying a weighted distance factor to the nearest four grid cells (Wu et al. 2018; Zhang et al. 2017).

The MOD09A1 surface reflectance data product (Collection 6) at 500-m spatial resolution and 8-day temporal resolution during 2008-2018 was used to calculate Enhanced Vegetation Index (EVI) and Land Surface Water Index (LSWI) (Zhang et al. 2017). We identified those observations affected by cloud, cloud shadow and aerosol as bad-quality observations, based on the quality assurance layer (QA) in the MOD09A1 dataset (Zhang et al. 2016). The bad-quality observations in the EVI time series data were gap-filled by applying the "Best Index Extraction Algorithm" (BISE) (Zhang et al. 2017). In this algorithm, a standard seasonal pattern for each pixel was first generated by extracting the median values of all the good-quality observations for each day of year (DOY) over 19 years (2000-2018). The data gaps were then filled with a linear interpolation and smoothed using a Savitzky-Golay filter (Zhang et al. 2017).

The MOD12Q1 land cover data product at 500-m spatial resolution during 2008-2018 was used in this study. The International Geosphere-Biosphere Programme (IGBP) land cover classification scheme in the MOD12Q1 data product includes croplands, forests, grasslands, and other land cover types. We aggregated the CDL dataset at 30-m spatial resolution to 500-m MODIS pixels and calculate the area percentages of all individual crop types (e.g., maize and soybean) within individual 500-m MODIS pixels. We further re-classify individual crop types by plant function types (C_3 and C_4 plant function types) and calculate the area percentages of C_3 and C_4 plant function types within each 500-m MODIS pixel.

2.5. GPP data from the Vegetation Photosynthesis Model

The VPM model is a light use efficiency (LUE) model and estimates daily GPP as a product of LUE and the amount of photosynthetically active radiation (PAR) absorbed by chlorophyll in the canopy ($APAR_{chl}$). The detailed description of the VPM model can be found in previous publications (Xiao et al. 2004a; Xiao et al. 2004b; Zhang et al. 2017). We used the improved VPM model (2.0), which considers both C_3 and C_4 crops and their areas within individual pixels (Wu et al. 2018; Zhang et al. 2017) .

$$GPP = APAR_{chl} * LUE \quad (1)$$

$$APAR_{chl} = FPAR_{chl} * PAR \quad (2)$$

$$LUE = LUE_0 * T_{scalar} * W_{scalar} \quad (3)$$

$$LUE_0 = LUE_{0-C3} * AF_{C3} + LUE_{0-C4} * AF_{C4} \quad (4)$$

where $FPAR_{chl}$ is the fraction of PAR absorbed by chlorophyll in the canopy; LUE_0 is the maximum light use efficiency under optimal environmental condition; T_{scalar} and W_{scalar} are the air temperature- and water- limitation scalar; AF_{C3} and AF_{C4} are the area fractions of C_3 and C_4 plants within a pixel (range from 0 - 1.0); $LUE_{0\text{-}C3}$ and $LUE_{0\text{-}C4}$ are the maximum LUE values for C_3 and C_4 plants, respectively.

A number of publications have reported the evaluation of GPP_{VPM} with GPP_{EC} estimates from the eddy flux tower sites, including maize (Dong et al. 2015; Kalfas et al. 2011), soybean (Jin et al. 2015; Wagle et al. 2015), winter wheat (Doughty et al. 2018; Yan et al. 2009) and paddy rice (Xin et al. 2017). All these publications reported strong agreement between GPP_{VPM} and GPP_{EC}, with a range of R^2 values from 0.70 to 0.98. We also ran VPM simulations with NCEP/NARR climate data, MODIS images and the CDL data to estimate 8-day GPP in the CONUS during 2008-2014 (Wu et al. 2018). We compared the resultant GPP_{VPM} with GPP simulated from the MOD17 algorithm (GPP_{MOD17}), CASA model (GPP_{CASA}), and SiBCASA model ($GPP_{SiBCASA}$) (Wu et al. 2018), and the results showed that GPP_{VPM} had the stronger relationships with GOME-2 solar-induced chlorophyll fluorescence (SIF) data in both normal years and drought year (2012) than do the other three GPP datasets.

In this study, we ran the VPM with NCEP/NARR climate data, MODIS images and the CDL data during 2008-2018 to estimate 8-day GPP (g C m^{-2} day^{-1}) at 500-m spatial resolution. For each pixel, it has 46 estimates of GPP_{VPM} in a year and we calculated annual sums of GPP_{VPM} for individual pixels. We also aggregated annual sums by crop types and their planted areas at county and national scales. The average annual GPP (GPP_{VPM_avg}) values of individual crop types (maize, soybean) in a county were calculated by the area fraction of specific crop type from the CDL datasets in each 500-m pixel. The total annual GPP (GPP_{VPM_Year}) (January - December) for a crop type for each county was calculated by multiplying GPP_{VPM_avg} with the total area of all those pixels with a specific crop located in the county.

2.6. MOD17 GPP dataset

The MOD17 GPP product (Running et al. 2004) is the most widely used global GPP data product. In this study we used MOD17A2H Collection 6 (GPP_{MOD17}) at the 500-m spatial resolution and 8-day temporal resolution. In the MOD17 data product, GPP is estimated as the product of LUE and the amount of PAR absorbed by the canopy ($APAR_{canopy}$) (Running et al. 2004). The land cover data product used in the model for MOD17A2H does not have information on C_3 and C_4 croplands, and the model parameter look-up table has applied only one LUE_0 (~1.04 g C MJ^{-1}) for crop GPP simulations (Wu et al. 2018). For simple comparison purpose, we also calculated the average annual MOD17 GPP (GPP_{MOD17_avg}) values of individual crop types (maize, soybean) and the total annual GPP (GPP_{MOD17_Year}) (January - December) by county and state, based on the CDL crop type data.

2.7. Statistical analyses

Simple linear regression models were used to characterize the relationship between grain production and GPP, and between grain production and cropping areas at county and national scales, at a minimum 0.05 significance threshold (p-value). Model performance was evaluated using the coefficient of determination (R^2), bias and root mean square error (RMSE).

A number of studies have used the vegetation indices over time to predict grain yields of crops in a field or a county (Peng et al. 2018; Zhao and Lobell 2017). In this study, we used the cumulative GPP over time to predict grain production in a county. A simple linear regression model was used to assess the relationship between grain production and cumulative GPP over time at 8-day temporal resolution at county-scale (see Equation 5). The model was run at 8-day time step over a year across all the counties in the CONUS during 2008-2018. We calculated the averaged R^2 value among all the counties at each time step, and then plot the R^2 values as a function of time. Based on the time course of R^2 value in a year, we assess the performance of using cumulative GPP_{VPM} to predict grain production over time at county scale. This will address the research questions related to in-season grain production forecasting: (1) at what day in a year the model start to predict grain production at county scale with reasonable accuracy, and (2) to what degree weather and climate (e.g., drought, flood) affect the model prediction over years.

$$\text{Grain Production} = a * \sum_{1}^{t} (GPP_t \times k) + b, \quad t = 1, 2, 3, \ldots, 46 \tag{5}$$

where t is the number of time steps in a year, which ranges from 1 to 46, as time series GPP has 46 data points in a year; k is the number of days in each time step, k is equal to 8 days when t ranges from 1 to 45, and k is 5 (non-leap year) or 6 (leap year) when t is 46.

3. Results

3.1. Spatial-temporal changes of maize and soybean planted area and harvested area during 2008-2018

At the national scale, Fig. 1a,b shows the interannual variation of maize and soybean planted area from both CDL and NASS data and NASS harvested area in the CONUS from 2008 to 2018. Between the planted area estimates from the CDL and NASS datasets, there are very small differences for maize (0.4 - 6.5%) and for soybean (0.1 - 5.8%) (Fig. 1a, b), which supports the use of the CDL dataset as input data for model simulations. The differences between NASS planted area and harvested areas are also small, except 2012 for maize crop (Fig. 1a, b). We calculated the mean values of planted area and harvested area over years (excluding the drought year 2012) and the deviation (anomalies) to the mean values for individual years (Fig. 1c, d, e). The normalized anomalies of maize planted area from both CDL and NASS datasets have similar dynamics during 2008-2018 (Fig. 1c,d). The maize planted area gradually increased between 2008 and 2012 and varied moderately over 2013-2018 (Fig. 1c). Maize harvested area had a similar temporal dynamics as maize planted area (Fig. 1e). The normalized anomalies of soybean planted area from both CDL and NASS also have similar dynamics during 2008-2018 (Fig. 1c,d), varied slightly during 2008-2013 but started to have an increase since 2014 (Fig. 1d). The anomaly of soybean harvested area agreed well with that of soybean planted area with a smaller magnitude of variation.

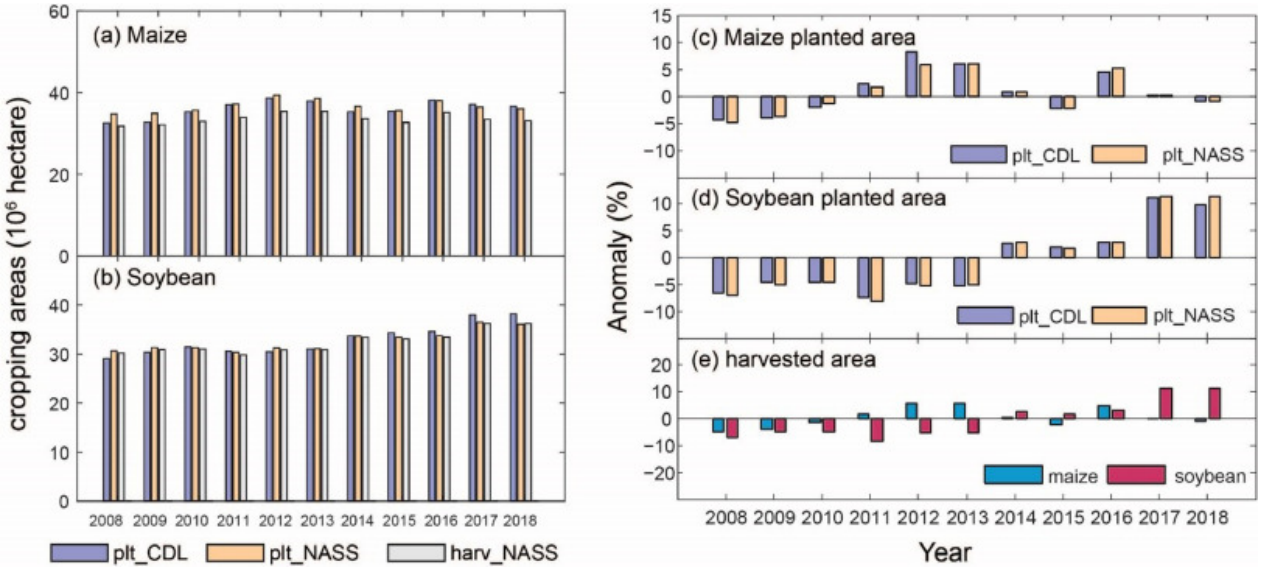

Download : Download high-res image (730KB) Download : Download full-size image

Figure 1. Interannual changes of planted area derived from CDL maps (plt_CDL), planted area from NASS statistics (plt_NASS), and harvested area from NASS statistics (harv_NASS) for a) maize and b) soybean; (c) normalized anomaly of planted area derived from CDL and NASS for maize; (d) normalized anomaly of planted area derived from CDL and NASS for soybean; (e)normalized anomaly of harvested area from NASS for maize and soybean.

At the county scale, Fig. 2 shows the spatial distributions of planted area and harvested area of maize and soybean crops in 2010 across all counties of the CONUS. There were strong spatial consistencies in planted areas between the CDL and NASS datasets in CONUS for both maize and soybean (Fig. 2), The CDL planted area estimates were highly consistent (only ~1% to 3% discrepancy) with NASS planted and harvested area estimates for both maize and soybean crops during 2008-2018 at the county and state scales (Fig. 3). The relationships between CDL planted area and NASS planted areas in individual years were relatively stable at the county scales (Table 1), with moderate differences in 2008 and 2009. These results further support the use of the CDL dataset as input data for model simulations.

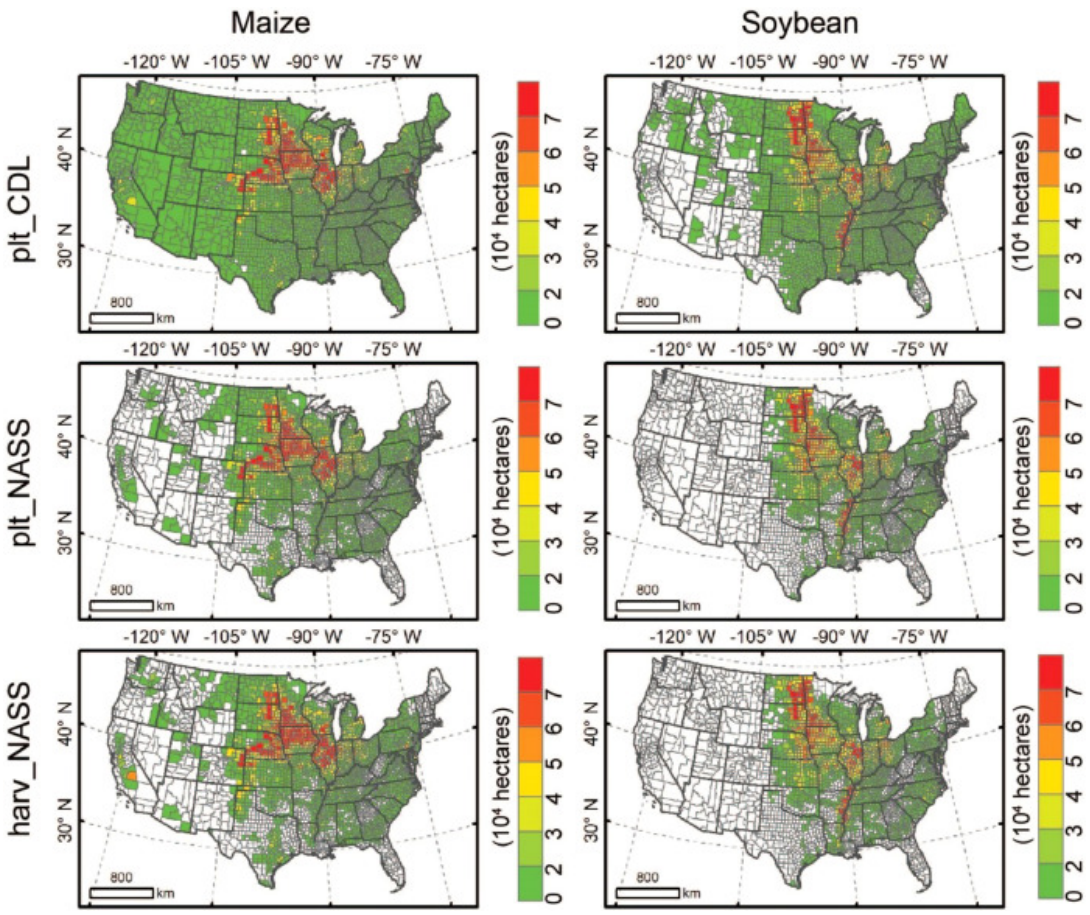

Download : Download high-res image (2MB) Download : Download full-size image

Figure 2. Spatial distribution of CDL planted area, NASS planted area, NASS harvested area, and NASS production over CONUS in 2010

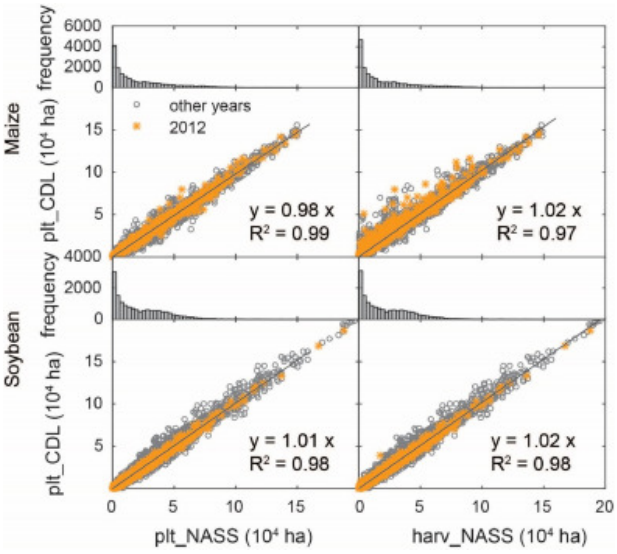

Download : Download high-res image (404KB) Download : Download full-size image

FEEDBACK

Figure 3. Relationship between NASS planted area, NASS harvested area and CDL planted area at the county scale from 2008-2018

Table 1. The summary statistics of simple linear regression models between the CDL planted area and the NASS planted area and harvested area of maize and soybean in the CONUS during 2008-2018 at the county scale. We used a simple linear regression model y = a * x. All the regression models have p-value < 0.001.

Year	Maize							
	plt_CDL vs plt_NASS				plt_CDL vs harv_NASS			
	slope	R^2	bias (ha)	RMSE (10^3 ha)	slope	R^2	bias (ha)	RMSE (10^3 ha)
2008	0.94	0.977	-1362.9	32.72	0.98	0.967	179.7	32.30
2009	0.93	0.984	-1349.7	32.63	0.97	0.975	-26.6	32.24
2010	0.98	0.990	-232.6	32.55	1.02	0.980	1034.6	32.16
2011	1.00	0.992	-62.2	34.59	1.04	0.977	1551.3	34.22
2012	0.98	0.990	-383.8	35.41	1.04	0.966	1660.2	34.64
2013	0.99	0.991	-361.0	35.67	1.03	0.977	1223.4	35.13
2014	0.97	0.990	-735.3	33.90	1.02	0.980	683.1	33.36
2015	0.99	0.992	-85.3	34.35	1.04	0.977	1426.7	33.88
2016	1.00	0.992	52.5	34.79	1.04	0.978	1548.5	34.37
2017	1.01	0.990	320.1	33.62	1.05	0.973	1813.9	33.19
2018	1.00	0.990	321.8	33.96	1.04	0.971	1819.5	33.55
Year	Soybean							
	plt_CDL vs plt_NASS				plt_CDL vs harv_NASS			
	slope	R^2	bias (ha)	RMSE (10^3 ha)	slope	R^2	bias (ha)	RMSE (10^3 ha)
2008	0.96	0.977	-1126.7	29.68	0.96	0.977	-1126.7	29.68
2009	0.98	0.980	-673.5	30.29	0.98	0.980	-673.5	30.29
2010	1.00	0.986	36.2	29.94	1.00	0.986	36.2	29.94
2011	1.03	0.986	193.4	29.88	1.03	0.986	193.4	29.88
2012	0.99	0.992	-490.5	29.70	0.99	0.992	-490.5	29.70
2013	1.01	0.988	12.8	30.73	1.01	0.988	12.8	30.73
2014	1.02	0.986	113.5	33.08	1.02	0.986	113.5	33.08
2015	1.02	0.985	666.5	33.04	1.02	0.985	666.5	33.04
2016	1.02	0.987	592.8	32.69	1.02	0.987	592.8	32.69
2017	1.03	0.982	1053.7	35.73	1.03	0.982	1053.7	35.73
2018	1.05	0.984	1573.8	35.77	1.05	0.984	1573.8	35.77

We further calculated the interannual trends of maize and soybean planted areas from the CDL and NASS datasets during 2008-2018 at the county scale (Fig. 4). A large number of counties in the NASS dataset do not have data for all the 11 years, and they were thus not included in the analysis of interannual trends of planted area. For those counties with continuous 11 years of maize and soybean planted area data, the spatial pattern of the interannual trends (slope values) from the NASS dataset has some similarity with that from CDL dataset (Fig. 4a,b,c,d). Based on the CDL dataset, interannual trends (slope values) of soybean planted area differed substantially from those of maize planted area (Fig. 4e,f). Out of 3107 counties with data in the CONUS, 2151 counties had an increasing trend of soybean planted area during 2008-2018, and 1857 counties had an increasing trend of maize planted area (Fig. 4e,f). In Illinois, maize planted area decreased while soybean planted area increased during 2008-2018. In the northern Great Plains, both maize and soybean planted areas increased in recent years (Fig. 4a,c).

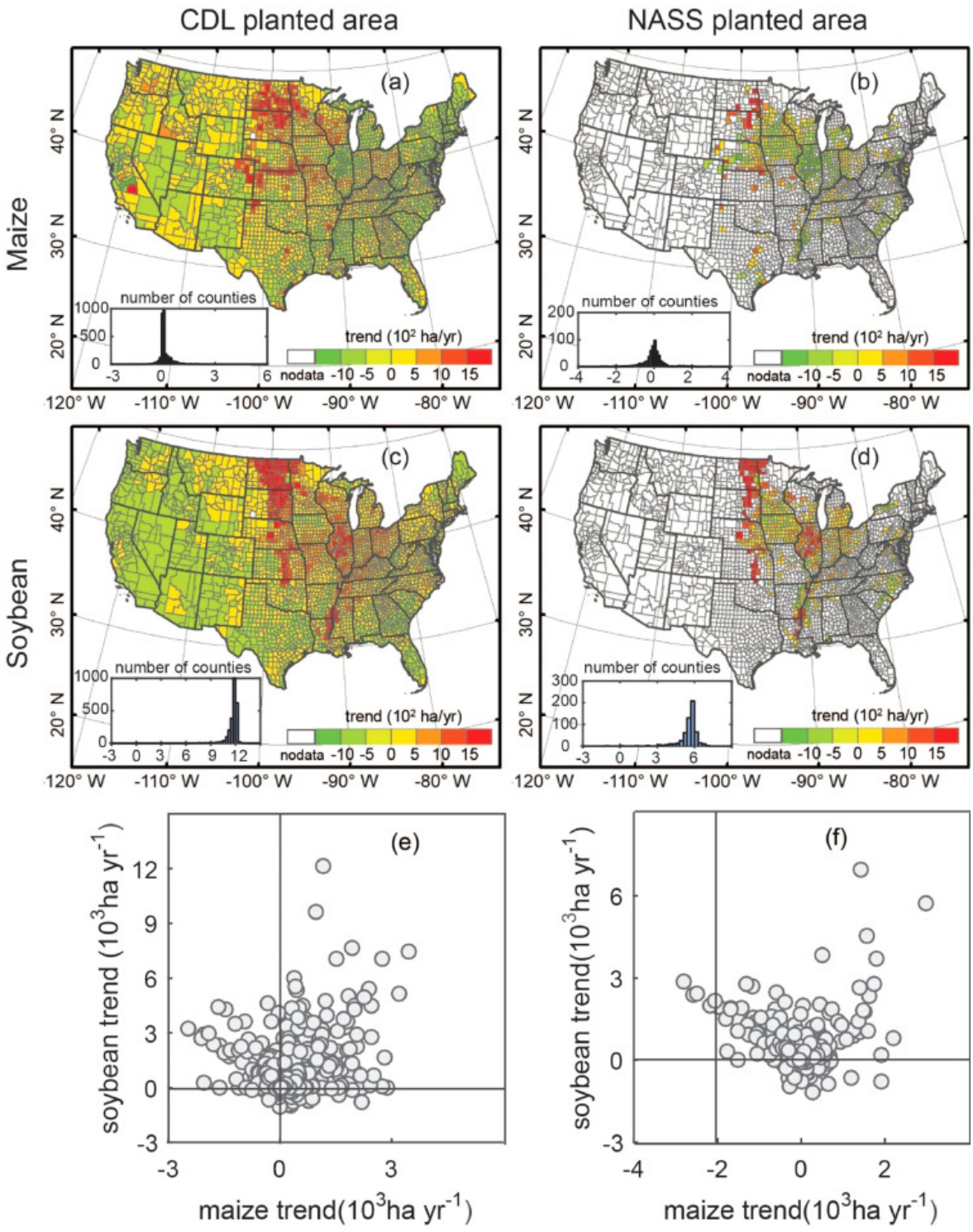

Download : Download high-res image (2MB) Download : Download full-size image

FEEDBACK

Figure 4. Interannual trend of (a) CDL planted area for maize; (b) NASS planted area for maize; (c) CDL planted area for soybean; (d) NASS planted area for soybean. (e) relationship between maize and soybean changing trend of CDL planted area (f) relationship between maize and soybean changing trend of NASS planted area

Fig. 5 shows the relationships among maize and soybean planted area, harvested area and grain production during 2008-2018 at the county scale. The slope values in the simple linear regression models represents the average yields (ton ha^{-1}) of maize and soybean in the CONUS during 2008-2018, which were calculated by either planted area or harvested area, and they have very small variations (Fig. 5). For maize, the average yields at the county scale (Table 2) among individual years had a small variation (< 10%), except for 2012. Because of heatwaves and drought in 2012, the average yield of maize in 2012 was 8.24 ton ha^{-1} at the county scale (Table 2), which is substantially (more than 20%) lower than multi-year average yields (10.7 ton ha^{-1} or 10.6 ton ha^{-1}). For soybean, the average yields at the county scale (Table 3) among individual years also had a small variation, and the 2012 drought resulted in ~10% drop in comparison to multi-year average yields. The results indicate that soybean crop was more resistant than maize crop in the 2012 severe drought.

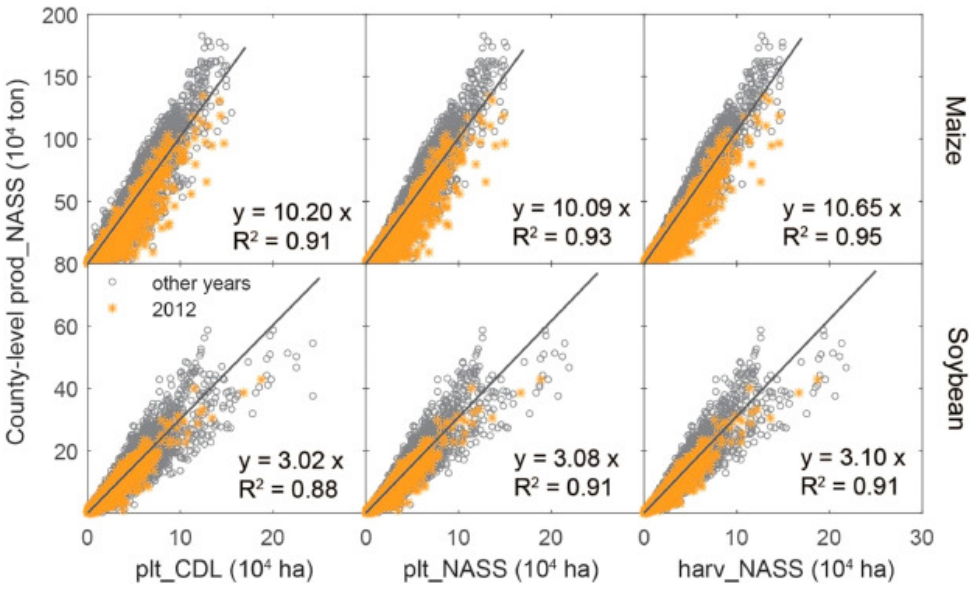

Download : Download high-res image (544KB) Download : Download full-size image

Figure 5. Relationship between NASS grain production, CDL planted area, NASS planted area, and NASS harvested area for maize and soybean at the county scale during 2008-2018

Table 2. The summary statistics of simple linear regression models between NASS grain production and crop planted and harvested areas for maize during 2008-2018 at the county scale. All the regression models have p-value < 0.001.

Year	Maize											
	prod_NASS vs plt_CDL				prod_NASS vs plt_NASS				prod_NASS vs harv_NASS			
	slope	R^2	bias (10^3 ton)	RMSE (10^3 ton)	slope	R^2	bias (10^3 ton)	RMSE (10^3 ton)	slope	R^2	bias (10^3 ton)	RMSE (10^3 ton)
2008	10.34	0.931	-14.11	344.52	9.83	0.950	-17.56	344.27	10.36	0.969	-12.77	348.85
2009	11.05	0.945	-12.45	362.17	10.43	0.963	-14.21	362.77	10.92	0.978	-10.10	366.68

2010	9.81	0.949	-14.31	329.46	9.71	0.961	-14.52	330.46	10.14	0.970	-10.42	333.61
2011	9.34	0.930	-16.05	339.13	9.37	0.942	-17.26	339.57	9.87	0.963	-12.17	344.40
2012	7.73	0.864	-12.24	290.68	7.63	0.867	-12.98	290.50	8.24	0.897	-9.82	294.77
2013	9.80	0.925	-7.39	359.88	9.73	0.940	-9.41	360.14	10.28	0.959	-5.56	364.24
2014	10.81	0.940	-7.16	373.26	10.57	0.952	-9.99	372.73	11.16	0.970	-6.67	376.55
2015	10.66	0.937	-14.20	379.85	10.64	0.952	-14.89	381.03	11.21	0.967	-10.32	385.29
2016	11.18	0.939	-18.98	406.71	11.22	0.953	-19.16	408.20	11.78	0.970	-14.43	412.94
2017	11.08	0.929	-15.84	390.59	11.23	0.946	-15.63	392.59	11.82	0.964	-11.15	397.27
2018	11.16	0.920	-16.33	397.86	11.31	0.943	-16.08	400.57	11.90	0.963	-11.52	405.55

Table 3. The summary statistics of simple linear regression models between NASS grain production and crop planted and harvested areas for soybean during 2008-2018 at the county scale. All the regression models have p-value < 0.001.

Year	Soybean											
	prod_NASS vs plt_CDL				prod_NASS vs plt_NASS				prod_NASS vs harv_NASS			
	slope	R^2	bias (ton)	RMSE (10^3 ton)	slope	R^2	bias (ton)	RMSE (10^3 ton)	slope	R^2	bias (ton)	RMSE (10^3 ton)
2008	2.76	0.894	828.19	82.71	2.68	0.926	-570.07	82.39	2.71	0.928	-491.39	82.50
2009	2.92	0.883	2260.98	89.25	2.89	0.921	807.65	89.09	2.93	0.925	853.93	89.20
2010	2.90	0.895	22.98	89.77	2.94	0.924	-794.78	89.93	2.97	0.926	-754.80	90.00
2011	2.68	0.843	1872.97	84.23	2.80	0.891	-59.08	83.99	2.83	0.898	37.05	84.20
2012	2.72	0.907	216.27	82.62	2.69	0.909	-422.19	82.24	2.72	0.914	-311.26	82.43
2013	2.88	0.894	1730.69	90.79	2.94	0.921	567.62	90.62	2.95	0.922	644.31	90.70
2014	3.10	0.901	1824.62	105.62	3.19	0.931	255.89	105.38	3.21	0.931	347.42	105.46
2015	3.16	0.896	-258.61	108.45	3.25	0.920	-323.39	109.11	3.28	0.923	-155.46	109.30
2016	3.40	0.919	110.10	114.83	3.51	0.948	-457.77	115.32	3.54	0.949	-373.80	115.41
2017	3.13	0.885	1413.64	116.07	3.27	0.910	1161.90	116.66	3.28	0.911	1235.02	116.73
2018	3.28	0.877	63.52	124.04	3.48	0.904	29.68	124.89	3.51	0.906	260.35	125.12

3.2. The relationship between GPP_{VPM} and NASS grain production during 2008-2018

At the CONUS scale, Fig. 6a,b shows the interannual variations of grain production from the NASS data and annual total GPP from the VPM model (GPP_{VPM_Year}). We calculated the deviation (anomaly) of annual grain production and GPP_{VPM} to the mean values during the study period except 2012 (Fig. 6c,d). The normalized anomaly of grain production show that maize grain production started to increase in 2013 (Fig. 6c) and soybean grain production started to increase in 2014 (Fig. 6d). In 2012, maize planted area (Fig. 1c) and harvested area (Fig. 1e) were higher than the multi-year mean values, but maize grain production in 2012 was substantially lower than the multi-year mean value, which highlights the substantial impacts of drought and heatwaves in 2012 on maize grain yield.

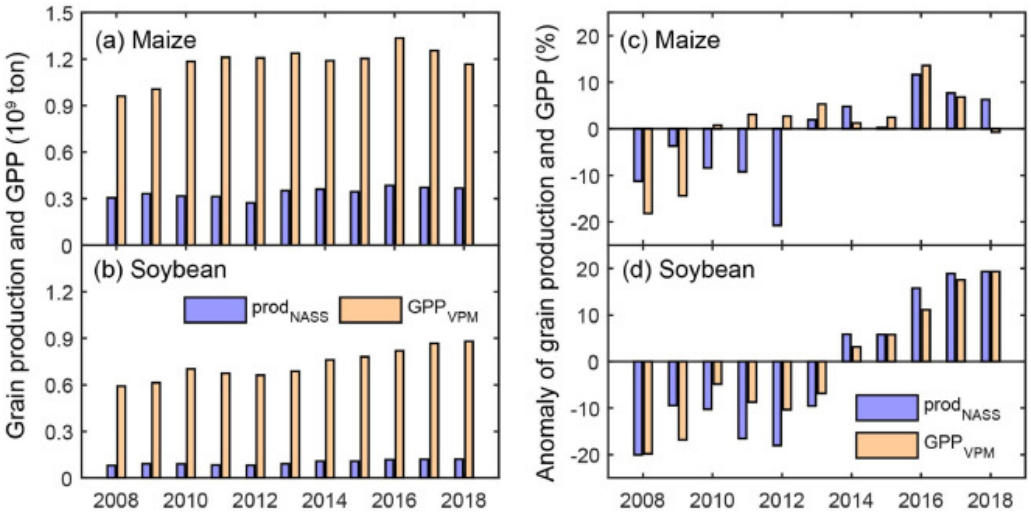

Download : Download high-res image (476KB)

Download : Download full-size image

Figure 6. Annual national grain production and total GPP_{VPM} for a) maize and b) soybean; (c) normalized anomaly of grain production and total GPP_{VPM} for maize (d) normalized anomaly of grain production and total GPP_{VPM} for soybean

Fig. 7a,b shows the spatial distributions of GPP_{VPM} and grain production at 500-m and county scales in the CONUS in 2010. At the county scale, the spatial distribution of GPP_{VPM_Year} was highly consistent with the spatial distributions of NASS grain production (Fig. 7c,d,e,f), planted area and harvested areas (Fig. 2). For maize croplands, the regions with the high GPP_{VPM} occurred in the Midwest. For soybean croplands, the regions with high GPP_{VPM_Year} occurred in the Midwest region and along the Mississippi delta area.

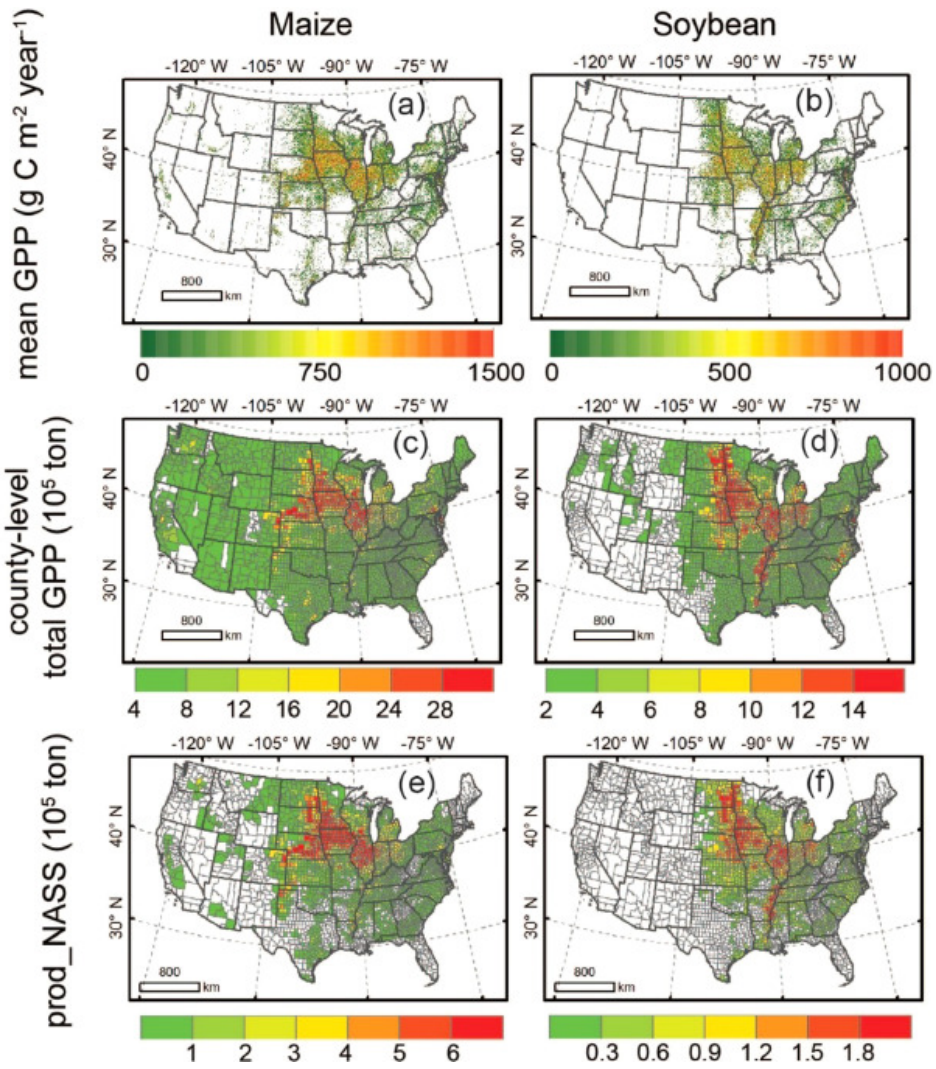

Download : Download high-res image (2MB) Download : Download full-size image

Figure 7. Spatial distributions of annual maize and soybean GPP simulated by VPM in 2010 at county scale. upper panel—mean annual GPP at a spatial resolution of 500-m; middle panels—annual total GPP at county scale; lower panels—NASS production at county scale. Annual total GPP at the county scale is calculated as the product of the mean GPP and CDL planted areas of maize and soybean in a county in 2010.

Fig 8 showed the interannual trends of maize and soybean grain production and GPP_{VPM_Year} at individual counties in the CONUS during 2008-2018. Among those counties that have 11-years of data from both the NASS statistics data and GPP_{VPM_Year} estimates, there are good agreements in their spatial distributions (Fig 8a,b,c,d). For maize, the hot-spots of grain production and GPP_{VPM_Year} increases over years occurred mostly in the Mid-west region. For soybean croplands, the hot-spots of grain production and GPP_{VPM_Year} increases over years occurred in the Mid-west region and the Northern Great Plains. Note that a large number of counties in the CONUS had experienced decreasing trends of maize grain production during 2008-2018.

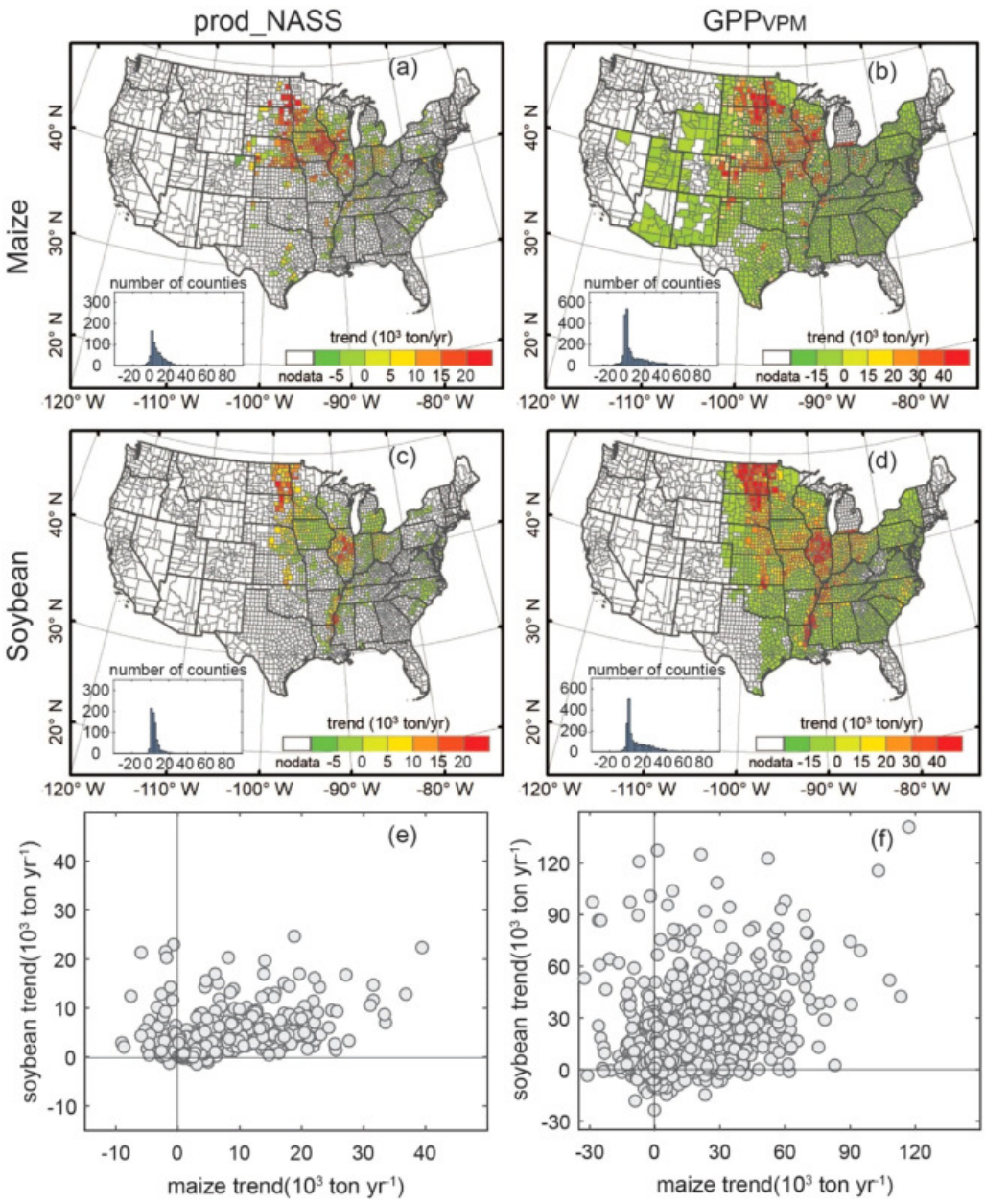

Download : Download high-res image (2MB) Download : Download full-size image

Figure 8. Interannual trend of (a) NASS production for maize; (b) annual total GPP_{VPM} for maize; (c) NASS production for soybean; (d) annual total GPP_{VPM} for soybean. (e) relationship between maize and soybean changing trend of NASS production (f) relationship between maize and soybean changing trend of annual total GPP_{VPM}

Fig. 9 shows the relationship between NASS grain production and GPP_{VPM_Year} (and GPP_{MOD17_Year}) for maize and soybean in the CONUS during 2008-2018 at the county scale. The slope values in the simple linear regression models represent the average harvest index (HI_{GPP}) of maize and soybean in the CONUS during 2008-2018 at the county scale. For maize crop, GPP_{VPM_Year} during 2008-2018 explained the 93% variation of NASS grain production at the county scale, with an average $HI_{GPP\text{-}VPM}$ of 0.31 (Fig. 9a). Because of severe drought in 2012, $HI_{GPP\text{-}VPM}$ in 2012 (0.25) was substantially (19%) lower than the average $HI_{GPP\text{-}VPM}$ (0.31), but R^2 value was still relatively high (R^2 = 0.89, p-value <0.001) (Table 4). For soybean crop, GPP_{VPM_Year} during 2008-2018 explained the 91% variation of NASS grain production at the county scale with an average $HI_{GPP\text{-}VPM}$ of 0.13 (Fig. 9b). The $HI_{GPP\text{-}VPM}$ in 2012 (0.12) was similar to 2011 but slightly lower than other years (0.12 - 0.14) (Table 4). In comparison, GPP_{MOD17_Year} also had strong relationships with NASS grain production at the county scale (Fig. 9c,d). For soybean crop (C_3 plant), $HI_{GPP\text{-}}$

$_{MOD17}$ (~0.18) values are moderately larger than $HI_{GPP\text{-}VPM}$ (0.14). However, for maize crop (C_4 plant), $HI_{GPP\text{-}MOD17}$ values (0.60) are substantially larger than $HI_{GPP\text{-}VPM}$ (0.31) at the county scale (Fig. 9).

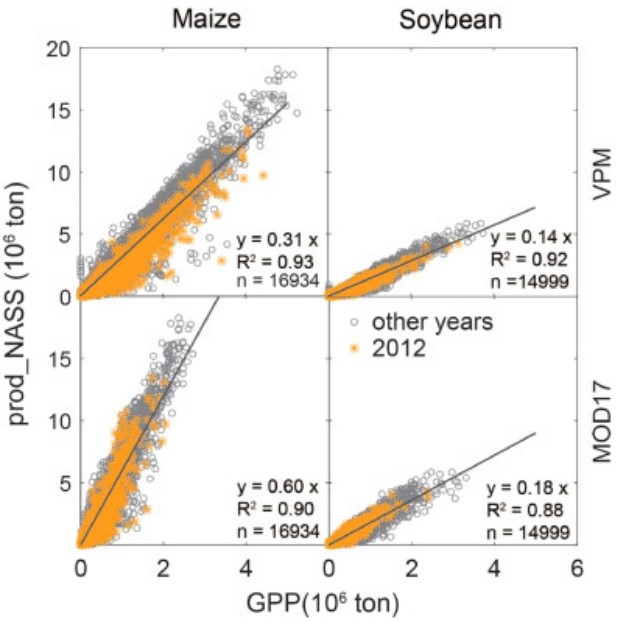

Download : Download high-res image (336KB) Download : Download full-size image

Figure 9. Relationships between NASS grain production and annual total GPP from VPM and MOD17 datasets in the CONUS during 2008-2018 at the county scale. Annual total GPP is calculated as the product of the mean GPP and CDL planted areas of maize and soybean in a county. The black solid line is the linear regression line for all the data during 2008-2018. All statistics with $p < 0.001$.

Table 4. The summary statistics of simple linear regression models between NASS grain production and annual total GPP from VPM and MOD17 datasets for maize and soybean during 2008-2018 at the county scale. All regression models have p-value < 0.001.

Year	VPM							
	Maize				Soybean			
	slope	R^2	bias (10^3 ton)	RMSE (10^3 ton)	slope	R^2	bias (10^3 ton)	RMSE (10^3 ton)
2008	0.33	0.926	-14.60	350.79	0.14	0.898	-1.00	82.22
2009	0.36	0.955	-13.42	362.46	0.15	0.920	-1.00	87.74
2010	0.29	0.943	-14.09	329.04	0.14	0.930	-3.05	88.48
2011	0.28	0.950	-15.84	341.11	0.13	0.919	-2.19	83.09
2012	0.25	0.891	-16.03	290.61	0.13	0.921	-2.23	81.25
2013	0.31	0.954	-12.26	359.62	0.14	0.934	-1.84	89.23
2014	0.32	0.965	-9.79	374.19	0.15	0.949	-2.94	103.68
2015	0.31	0.950	-15.65	380.38	0.15	0.914	-4.07	106.25
2016	0.32	0.945	-19.88	406.84	0.15	0.928	-3.72	112.72

2017	0.33	0.933	-19.56	388.70	0.15	0.914	-3.79	113.11
2018	0.33	0.948	-20.02	398.62	0.15	0.922	-4.34	122.18
Year	MOD17							
	Maize				Soybean			
	slope	R^2	bias (10^3 ton)	RMSE (10^3 ton)	slope	R^2	bias (10^3 ton)	RMSE (10^3 ton)
2008	0.59	0.907	-18.98	339.18	0.15	0.878	-2.45	74.54
2009	0.62	0.921	-16.83	357.01	0.16	0.877	-1.22	80.78
2010	0.55	0.919	-14.40	326.75	0.16	0.914	-2.56	82.46
2011	0.57	0.918	-14.46	338.97	0.16	0.862	-0.51	77.51
2012	0.53	0.820	-16.08	284.75	0.17	0.879	-1.95	75.10
2013	0.60	0.916	-10.58	357.09	0.17	0.904	-1.18	83.05
2014	0.65	0.932	-10.92	370.25	0.18	0.903	-1.57	96.47
2015	0.62	0.911	-16.75	375.58	0.18	0.889	-3.91	98.46
2016	0.60	0.925	-21.20	403.72	0.18	0.912	-3.40	104.84
2017	0.62	0.909	-21.68	384.69	0.17	0.879	-2.73	105.24
2018	0.66	0.910	-22.43	392.83	0.18	0.882	-4.08	112.80

3.3. In-season relationships between cumulative GPP and NASS grain production over time in a year during 2008-2018

In the CONUS, both maize and soybean are cultivated as single crop in a year at individual crop fields. Maize crops are usually planted in April through June and harvested in October and November. Soybean crops are usually planted in late April through June and harvested in September through November. For simplicity, we calculated cumulative GPP_{VPM} values (GPP_{VPM_CUM}) of maize and soybean in a county from January 1st at 8-day interval, and then we established the simple linear regression models that used NASS grain production (Y, dependent variable) and GPP_{VPM_CUM} (X, independent variable) over time (8-day interval) within a year (NASS grain production = a * GPP_{VPM_CUM} + b). We calculated average R^2 value of all counties for each time step and reported the R^2 values over each time step in a year (Fig. 10). According to the R^2 curve, the model prediction skill increases over time and reaches 90% by the end of July (Fig. 10), which is approximately one to two months before the start of harvesting time for soybean and maize crops. The model prediction skill showed slight differences among individual years. For maize, the prediction skill was slightly lower in 2008, 2009, and 2012 than in other years, which could be explained by the warm spring and summer drought in 2012 and the underestimation of planted areas in 2008 and 2009 from the CDL dataset. Similarly, for soybean, the prediction skill was slightly lower in 2008 and 2009 than in other years, but it was relatively stable in the drought 2012. In comparison, GPP_{MOD17_CUM} also showed very good prediction skills in most years for both maize and soybean, except for maize in 2012 (Fig. 10).

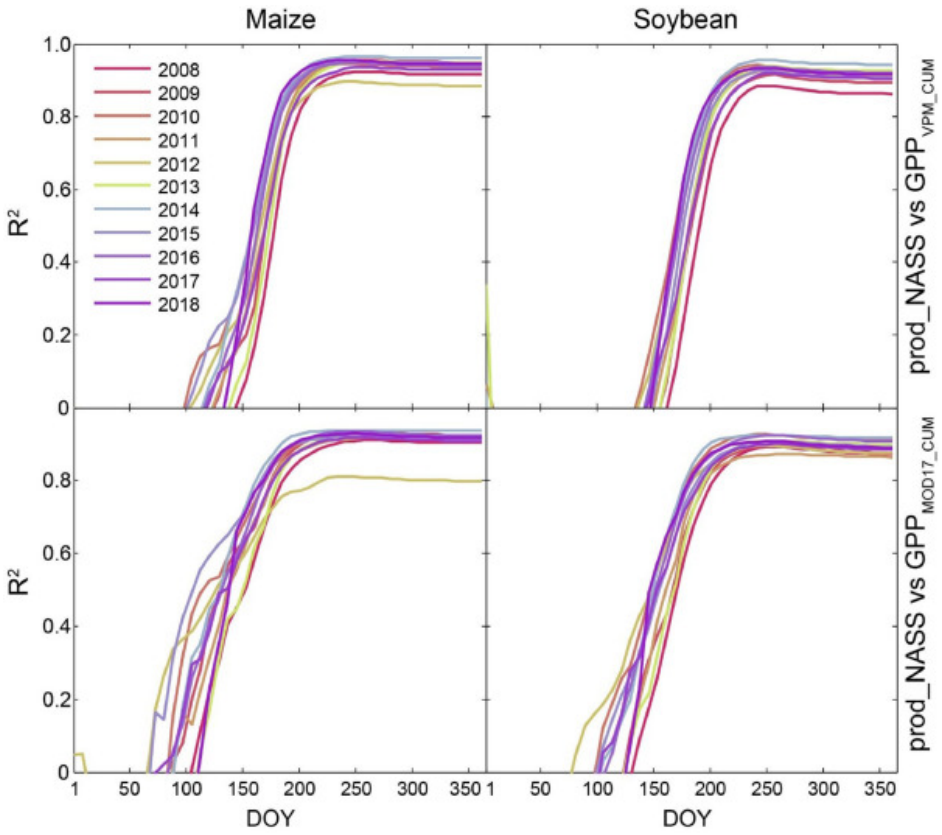

Download : Download high-res image (578KB)

Download : Download full-size image

Figure 10. The performance or skill (R^2 values) of simple linear regression models between NASS grain production and cumulated GPP of maize and soybean from VPM and MOD17 datasets over time (8-day temporal resolution) in a year during 2008-2018 over the CONUS.

4. Discussion

4.1. Maize and soybean planted and harvested areas from the CDL and NASS datasets

Satellite remote sensing has been widely used to identify and map cropland planted area in the CONUS (Cai et al. 2018; Massey et al. 2017; Wang et al. 2019; Zhong et al. 2014). The annual CDL datasets have high producer and user accuracies (~97%) for maize and soybean over CONUS. Such high classification accuracy was achieved by the machine learning image classification algorithm and large amounts of ground reference data used to train the algorithms. The training and validation ground reference data were sampled from USDA Farm Service Agency (FSA) Common Land Unit (CLU) database and its associated attributes reported by famers. Note that several global GPP data products, e.g., MOD17A2 (Running et al. 2004), have not considered the different photosynthetic capability of C_3 and C_4 crops and not incorporated the CDL dataset that contains information on individual crop types, which can partly explain that they underestimate GPP of maize and other C_4 crops (Guanter et al. 2014; Xin et al. 2013). Our previous study in the CONUS clearly show that the use the CDL dataset is essential for simulations of VPM and other data-driven models (Wu et al. 2018).

The spatial-temporal consistency of crop planted areas between the remote sensing approach (e.g., CDL) and the agricultural statistical approach (e.g., NASS) at administrative levels (e.g., county, state, nation) has been an important research topic among both agricultural and remote sensing communities (Cai et al. 2018; Wang et al. 2019). Previous studies reported good agreement between the CDL and NASS planted area data in 2009 (Boryan et al. 2011; USDA, 2018). Our study also shows that the CDL crop planted area estimates had good spatial-temporal consistency with the NASS planted area estimates at county and national scales during 2008-2018. The NASS agricultural statistics uses stratification methods to classify land into differe

intensity groups or strata based on percent cultivation in a given land parcel, which provides the area sampling frames (Boryan and Yang 2017). In 2010, an automatic stratification method based on the CDL dataset was developed and used in several states (Boryan et al. 2014), which significantly improved stratification accuracies in intensively cropped areas and performed less well in non-agricultural areas as compared with the land cover map method. Recently, an integrated automated stratification and traditional manual hybrid stratification process was implemented in NASS area frame operations (Boryan and Yang 2017), which may further improve the NASS dataset in the near future.

Our study demonstrates the potential of the CDL and NASS statistic datasets in understanding the changes of planted area, harvested area, and grain production of maize and soybean in the CONUS during 2008-2018. Over these years, maize and soybean planted areas in the CONUS were not affected by summer drought but did increase in response to international demand and grain price in late 2010s. However, maize harvested area and grain production in the CONUS was substantially reduced in 2012 with severe summer drought, particularly in the Midwest states. As the climate models predict larger climate variation and more frequent and severe drought in the years to come (Dai 2012; IPCC 2013; Trenberth et al. 2013), how to improve the resilience of maize and soybean crops to climate variation and change would be a major challenge for the farmers and the society.

4.2. Harvest Index – The relationships between GPP, AGB and NASS grain production of maize and soybean

Gross primary production (GPP), net primary production (NPP) and aboveground biomass (AGB) are related to grain yield (ton ha^{-1}) and production (ton). The "Harvest Index" (HI) is widely used term (Hay 1995) and often defined across various scales from plants to fields, and county as the ratio between crop grain yield (ton ha^{-1}) and aboveground biomass (AGB), namely HI_{AGB}. Grain yield of individual plants is affected by two processes: (1) flowering and pollination, which affects grain number, and (2) grain-filling, which determines individual grain sizes. Many studies have shown that these two processes are highly sensitive to heat and drought stresses (Guan et al. 2016; Liu et al. 2008; Lobell et al. 2014). Many studies reported that HI_{AGB} values often vary substantially among individual crop types, for example, 0.25 – 0.58 for maize (Guan et al. 2016), and 0.30 – 0.44 for soybean (Johnson and Major 1979; Krisnawati and Adie 2015; Lobell et al. 2002; Monfreda et al. 2008), which could be attributed to large degree how and when maize and soybean plants were harvested and AGB was measured.

Harvest Index can also be defined as the ratio between NASS crop grain production and gross primary production, namely HI_{GPP}. In a study on croplands in Montana (He et al. 2018), GPP data from the data-driven model during 2008-2015 and calibrated HI_{GPP_MOD17} (0.44) were used to estimate maize grain production, and resultant GPP-derived grain production had a strong linear relationship with NASS grain production for maize at the county scale ($R^2 = 0.82$). Our study shows that GPP_{VPM_Year} data during 2008-2018 were strongly correlated with NASS grain production (GP) data for maize ($GP = 0.31 * GPP_{VPM\_Year}$, $R^2 = 0.93$) and soybean ($GP = 0.14 * GPP_{VPM\_Year}$, $R^2 = 0.91$) at the county scale over the CONUS (Fig. 9). HI_{GPP} of maize, which is the slope of the simple linear regression model between GP and GPP_{VPM_Year} of maize at the county scale in individual years, varied from 0.25 in the severe drought year (2012) to 0.36 in the wet year (2009) (Table 4). HI_{GPP} of soybean varied from 0.12 in the drought year (2012) to 0.14 in the wet year (2009) (Table 4). The interannual variations of HI_{GPP} in this study at the CONUS scale could come from multiple sources. Many studies have discussed the effects of environment, management and crop genetics (variety) (Erickson et al. 2017; Licht et al. 2019; Lobell and Azzari 2017). In this study, the environmental factors, for example, severe drought in 2012, have strong effect on GPP and maize grain production. Cropland management factors have affected planted and harvested area, for example, the differences of planted area between CDL and NASS datasets were larger in 2008 and 2009 than in other years (Table 1), which could lead to moderate variations of annual HI_{GPP} in those two years. It is well known that crop genetics (e.g., crop variety) affect crop grain yield and production, as some crop types and genotypes are more tolerance to drought and pathogens, and more sensitive to changing crop management, like narrow row spacing and application of more modern managing technique. However, as HI_{GPP} values of maize and soybean have relatively moderate interannual variations during "normal" years, it clearly indicates the potential of using HI_{GPP} and GPP_{VPM} data to estimate maize and soybean grain production over those "normal" years at the county scale. Additional efforts are needed to elucidate the relationships between GPP and NASS grain production at those individual farms used in the NASS crop surveys, which could further reduce the spatial-temporal variations of harvest index (HI_{GPP}) for maize and soybean crops.

4.3. Prediction of maize and soybean grain production by GPP at the county scale

Numerous studies have used vegetation indices to predict crop grain yields (Bolton and Friedl 2013; Zhao et al. 2015). A number of LUE models estimate daily GPP of croplands (He et al. 2018; Yuan et al. 2007; Zhang et al. 2017). Several studie

GPP data to estimate crop grain yields by assuming that yield is a function of GPP, autotrophic respiration, HI_{AGB} and the root to shoot ratio (Guan et al. 2016; Marshall et al. 2018; Yuan et al. 2016). These studies compared the resultant yield estimate with the yield data from the flux tower sites (Yuan et al. 2016), and NASS yield data in the Midwest Corn-Belt (Guan et al. 2016) and the CONUS (Marshall et al. 2018). These studies include maize, soybean, and winter wheat, and reported moderate relationships between NASS grain yield data and modeled yield estimates (R^2 ranging from 0.5 to 0.7) at the county and state scales (Guan et al. 2016; Marshall et al. 2018). As NASS crop grain yield data at the county scale were derived from the survey and sampling approach, more studies are needed to compare yield data at individual farms or fields used in the NASS crop surveys.

In our study, we focused on the relationship between GPP and NASS grain production of maize and soybean in the CONUS at the county scale. In an initial effort to explore the potential of in-season forecasting, we calculated the simple linear regression model between cumulative GPP_{VPM_CUM} over time at 8-day interval and annual NASS grain production at the county scale, and the simple linear regression model was able to account for more than 80% of variation of NASS grain production of maize and soybean among all the counties in the CONUS by the end of June, and more than 90% by the end of July (Fig. 10). Peng et al. (2018) incorporated satellite derived EVI and climate forecast data in a crop model to forecast U.S. maize yield, they also found EVI improved the forecasting significantly in July and August. Therefore, the satellite-based information can play an important role in early crop yield and production forecast.

The capacity of in-season forecasting of grain production can be further improved in several aspects. First, the GPP_{VPM} simulation in this study was carried out at a moderate spatial resolution (500-m), and it could be improved by using high spatial resolution images (e.g., 30-m Landsat, and 10-m Sentinel-2 and Sentinel-1). Second, in this study we used the annual maps of crop types and planted areas from the CDL dataset at 30-m spatial resolution. Note that the CDL dataset took time to generate and was often released in the spring of next year (one-year delay). Although it is okay to assume relatively small changes of maize and soybean planted areas between two years and use previous-year CDL dataset for initial simulation of VPM model, simulations of VPM and in-season forecasting of crop grain production could be certainly improved if in-season maps of crop type (e.g., maize, soybean), planted area and harvested area at high spatial resolutions (e.g., 30-m or 10-m) are also generated and available to the public. Numerous studies have been done for identifying and mapping individual crop types in the growing season using single image (Van Niel and McVicar 2004; Yang et al. 2011) or multiple images (Chang et al. 2007; Foerster et al. 2012). Recently, a few studies reported their efforts for in-season crop mapping at high spatial resolutions (Cai et al. 2018; Wang et al. 2020; Wang et al. 2019). It remains to be a major challenge for the remote sensing community to develop in-season maps of crop types, planted areas and harvested areas in the CONUS.

5. Conclusion

Our study thoroughly reported the spatial-temporal dynamics of NASS crop statistical data (crop planted area, harvested area, grain production), satellite-based CDL crop planted area, and GPP estimates from the VPM model at the county and national scale during 2008-2018. There are strong spatial-temporal consistencies between the planted area from the CDL dataset and NASS crop statistics during 2008–2018 at the county scale, which supports the use of the CDL dataset by models. For maize and soybean crops, the HI_{GPP} values, which is calculated as the ratio between NASS grain production and GPP at the county scale, have relatively small variations over years during 2008-2018, except the extreme drought year (2012). Cumulative GPP_{VPM} and GPP_{MOD17} over time at 8-day interval within the maize and soybean growing season, together with HI_{GPP}, were able to explain and predict grain production of maize and soybean at the county scale about 1-2 month ahead of crop harvest. The strong and robust linear relationships between cumulative GPP_{VPM} and NASS grain production of maize and soybean in the CONUS at the county scale highlight the potential of GPP_{VPM} in monitoring maize and soybean grain production in the CONUS.

Authors' contribution

X. X. and X. W. designed the study. Z.Y. provided the CDL planted acreage estimates. X. W. ran the VPM model and analyzed the data. All authors contributed to the result interpretation and discussion. X.W. and X.X led the writing of the manuscript, and all co-authors reviewed and edited the manuscript.

Declaration of Competing Interest

The authors declare that they have no known competing financial interests or personal relationships that could have appeared to influence the work reported in this paper.

Acknowledgements

This study was supported by research grants through the USDA National Institute of Food and Agriculture (NIFA) (2013-69002 and 2016-68002-24967) and the US National Science Foundation EPSCoR program (IIA-1301789, IIA-1920946), the US National Science Foundation grant (IIA-1946093) and the NASA-funded Geostationary Carbon Cycle Observatory (GeoCarb) Mission (GeoCarb Contract # 80LARC17C0001). We thank two anonymous reviewers for their constructive comments and suggestions on the earlier versions of the manuscript.

Recommended articles Citing articles (0)

References

Atzberger, 2013 C. Atzberger
Advances in Remote Sensing of Agriculture: Context Description, Existing Operational Monitoring Systems and Major Information Needs (vol 5, pg 949, 2013)
Remote Sensing, 5 (2013), p. 4124
4124
CrossRef View Record in Scopus Google Scholar

Becker-Reshef et al., 2010 I. Becker-Reshef, E. Vermote, M. Lindeman, C. Justice
A generalized regression-based model for forecasting winter wheat yields in Kansas and Ukraine using MODIS data
Remote Sensing of Environment, 114 (2010), pp. 1312-1323
Article Download PDF View Record in Scopus Google Scholar

Belgiu and Csillik, 2018 M. Belgiu, O. Csillik
Sentinel-2 cropland mapping using pixel-based and object-based time-weighted dynamic time warping analysis
Remote Sensing of Environment, 204 (2018), pp. 509-523
Article Download PDF View Record in Scopus Google Scholar

Bolton and Friedl, 2013 D.K. Bolton, M.A. Friedl
Forecasting crop yield using remotely sensed vegetation indices and crop phenology metrics
Agricultural and Forest Meteorology, 173 (2013), pp. 74-84
Article Download PDF View Record in Scopus Google Scholar

Boryan and Yang, 2017 C. Boryan, Z. Yang
Integration of the cropland data layer based automatic stratification methods into the traditional area frame construction process
Survey Research Methods, 11 (2017), pp. 289-306
View Record in Scopus Google Scholar

Boryan et al., 2014 C. Boryan, Z. Yang, L. Di, K. Hunt
A New Automatic Stratification Method for U.S. Agricultural Area Sampling Frame Construction Based on the Cropland Data Layer
Ieee Journal of Selected Topics in Applied Earth Observations and Remote Sensing, 7 (2014), pp. 4317-4327
CrossRef View Record in Scopus Google Scholar

Boryan et al., 2011 C. Boryan, Z. Yang, R. Mueller, M. Craig
Monitoring US agriculture: the US Department of Agriculture, National Agricultural Statistics Service, Cropland Data Layer Program
Geocarto International, 26 (2011), pp. 341-358
CrossRef View Record in Scopus Google Scholar

Burke and Lobell, 2017 M. Burke, D.B. Lobell
Satellite-based assessment of yield variation and its determinants in smallholder African systems
Global and time-resolved monitoring of crop photosynthesis with chlorophyll fluorescence, 114 (9) (2017), pp. 2189-2194
CrossRef View Record in Scopus Google Scholar

Cai et al., 2018 Y. Cai, K. Guan, J. Peng, S. Wang, C. Seifert, B. Wardlow, Z. Li
A high-performance and in-season classification system of field-level crop types using time-series Landsat data and a machine learning approach
Remote Sensing of Environment, 210 (2018), pp. 35-47
Article Download PDF View Record in Scopus Google Scholar

Chang et al., 2007 J. Chang, M.C. Hansen, K. Pittman, M. Carroll, C. DiMiceli
Corn and soybean mapping in the united states using MODIS time-series data sets
Agronomy Journal, 99 (6) (2007), pp. 1654-1664
CrossRef View Record in Scopus Google Scholar

Dai, 2012 A. Dai
Increasing drought under global warming in observations and models
Nature Climate Change, 3 (2012), pp. 52-58
View Record in Scopus Google Scholar

Dong et al., 2015 J.W. Dong, X.M. Xiao, P. Wagle, G.L. Zhang, Y.T. Zhou, C. Jin, M.S. Torn, T.P. Meyers, A.E. Suyker, J.B. Wang, H.M. Yan, C. Biradar, B. Moore
Comparison of four EVI-based models for estimating gross primary production of maize and soybean croplands and tallgrass prairie under severe drought
Remote Sensing of Environment, 162 (2015), pp. 154-168
Article Download PDF View Record in Scopus Google Scholar

Doraiswamy et al., 2003 P.C. Doraiswamy, S. Moulin, P.W. Cook, A. Stern
Crop yield assessment from remote sensing
Photogrammetric Engineering and Remote Sensing, 69 (2003), pp. 665-674
CrossRef View Record in Scopus Google Scholar

Doughty et al., 2018 R. Doughty, X. Xiao, X. Wu, Y. Zhang, R. Bajgain, Y. Zhou, Y. Qin, Z. Zou, H. McCarthy, J. Friedman, P. Wagle, J. Basara, J. Steiner
Responses of gross primary production of grasslands and croplands under drought, pluvial, and irrigation conditions during 2010–2016, Oklahoma, USA
Agricultural Water Management, 204 (2018), pp. 47-59
Article Download PDF View Record in Scopus Google Scholar

Erickson et al., 2017 Erickson, B., Lowenberg-Deboer, J., & Bradford, J. (2017). 2017 precision agriculture dealership survey.
Google Scholar

Foerster et al., 2012 S. Foerster, K. Kaden, M. Foerster, S. Itzerott
Crop type mapping using spectral-temporal profiles and phenological information
Computers and Electronics in Agriculture, 89 (2012), pp. 30-40
Article Download PDF View Record in Scopus Google Scholar

Fritz et al., 2019 S. Fritz, L. See, J.C.L. Bayas, F. Waldner, D. Jacques, I. Becker-Reshef, A. Whitcraft, B. Baruth, R. Bonifacio, J. Crutchfield, F. Rembold, O. Rojas, A. Schucknecht, M. Van der Velde, J. Verdin, B. Wu, N. Yan, L. You, S. Gilliams, S. Mücher, R. Tetrault, I. Moorthy, I. McCallum
A comparison of global agricultural monitoring systems and current gaps
Agricultural Systems, 168 (2019), pp. 258-272
Article Download PDF View Record in Scopus Google Scholar

Gardiner 2016 Gardiner

U.S. Agriculture Exports: Recent Trends and Commodity Exposure to International Trade

Economic Report, FCA – ORP – AEPT (2016)

Google Scholar

Guan et al., 2016 K. Guan, J.A. Berry, Y. Zhang, J. Joiner, L. Guanter, G. Badgley, D.B. Lobell

Improving the monitoring of crop productivity using spaceborne solar-induced fluorescence

Global Change Biology, 22 (2016), pp. 716-726

CrossRef View Record in Scopus Google Scholar

Guanter et al., 2014 L. Guanter, Y. Zhang, M. Jung, J. Joiner, M. Voigt, J.A. Berry, C. Frankenberg, A.R. Huete, P. Zarco-Tejada, J.E. Lee, M.S. Moran, G. Ponce-Campos, C. Beer, G. Camps-Valls, N. Buchmann, D. Gianelle, K. Klumpp, A. Cescatti, J.M. Baker, T.J. Griffis

Global and time-resolved monitoring of crop photosynthesis with chlorophyll fluorescence

Proceedings of the National Academy of Sciences of the United States of America, 111 (14) (2014), pp. E1327-E1333

CrossRef View Record in Scopus Google Scholar

Han et al., 2012 W.G. Han, Z. Yang, L.P. Di, R. Mueller

CropScape: A Web service based application for exploring and disseminating US conterminous geospatial cropland data products for decision support

Computers and Electronics in Agriculture, 84 (2012), pp. 111-123

Article Download PDF View Record in Scopus Google Scholar

Hay, 1995 R.K.M. Hay

Harvest Index - a Review of Its Use in Plant-Breeding and Crop Physiology

Annals of Applied Biology, 126 (1995), pp. 197-216

CrossRef View Record in Scopus Google Scholar

He et al., 2018 M. He, J. Kimball, M.P. Maneta, B. Maxwell, A. Moreno, S. Begueria, X. Wu

Regional crop gross primary productivity and yield estimation using fused Landsat-MODIS data

Remote Sensing, 10 (2018), p. 372

CrossRef View Record in Scopus Google Scholar

Iizumi and Ramankutty, 2015 T. Iizumi, N. Ramankutty

How do weather and climate influence cropping area and intensity

Global Food Security, 4 (2015), pp. 46-50

Article Download PDF View Record in Scopus Google Scholar

IPCC 2013 IPCC

Climate change 2013: The Physics Science Basis. Contribution of Working Group I to the Fifth Assessment Report of the Intergovenmental Panel on Climate Change

Tech. rep., IPCC, Cambridge University Press, New York, NY, USA (2013)

2013

Google Scholar

Jin et al., 2015 C. Jin, X.M. Xiao, P. Wagle, T. Griffis, J.W. Dong, C.Y. Wu, Y.W. Qin, D.R. Cook

Effects of in-situ and reanalysis climate data on estimation of cropland gross primary production using the Vegetation Photosynthesis Model

Agricultural and Forest Meteorology, 213 (2015), pp. 240-250

Article Download PDF View Record in Scopus Google Scholar

Johnson, 2016 D.M. Johnson

A comprehensive assessment of the correlations between field crop yields and commonly used MODIS products

International Journal of Applied Earth Observation and Geoinformation, 52 (2016), pp. 65-81

Article Download PDF View Record in Scopus Google Scholar

Johnson and Major, 1979 D.R. Johnson, D.J. Major
Harvest Index of Soybeans as Affected by Planting Date and Maturity Rating
Agronomy Journal, 71 (1979), pp. 538-541
CrossRef View Record in Scopus Google Scholar

Kalfas et al., 2011 J.L. Kalfas, X. Xiao, D.X. Vanegas, S.B. Verma, A.E. Suyker
Modeling gross primary production of irrigated and rain-fed maize using MODIS imagery and CO2 flux tower data
Agricultural and Forest Meteorology, 151 (2011), pp. 1514-1528
Article Download PDF View Record in Scopus Google Scholar

Krisnawati and Adie, 2015 A. Krisnawati, M. Adie
Variability of Biomass and Harvest Index from Several Soybean Genotypes as Renewable Energy Source
Energy Procedia, 65 (2015), pp. 14-21
Article Download PDF View Record in Scopus Google Scholar

Licht et al., 2019 M.A. Licht, M.R. Parvej, E.E. Wright
Corn Yield Response to Row Spacing and Plant Population in Iowa
Crop, Forage & Turfgrass Management, 5 (1) (2019), pp. 1-7
CrossRef Google Scholar

Liu et al., 2008 X. Liu, J. Jin, G. Wang, S.J. Herbert
Soybean yield physiology and development of high-yielding practices in Northeast China
Field Crops Research, 105 (2008), pp. 157-171
Article Download PDF View Record in Scopus Google Scholar

Lobell, 2013 D.B. Lobell
The use of satellite data for crop yield gap analysis
Field Crops Research, 143 (2013), pp. 56-64
Article Download PDF View Record in Scopus Google Scholar

Lobell and Azzari, 2017 D.B. Lobell, G. Azzari
Satellite detection of rising maize yield heterogeneity in the U.S. Midwest
Environmental Research Letters, 12 (2017), Article 014014
CrossRef View Record in Scopus Google Scholar

Lobell et al., 2002 D.B. Lobell, J.A. Hicke, G.P. Asner, C. Field, C. Tucker, S. Los
Satellite estimates of productivity and light use efficiency in United States agriculture, 1982-98
Global Change Biology, 8 (2002), pp. 722-735
View Record in Scopus Google Scholar

Lobell et al., 2014 D.B. Lobell, M.J. Roberts, W. Schlenker, N. Braun, B.B. Little, R.M. Rejesus, G. Hammer
Greater sensitivity to drought accompanies maize yield increases in the U.S. Midwest
Science, 344 (2014), pp. 516-519
CrossRef View Record in Scopus Google Scholar

Marshall et al., 2018 M. Marshall, K. Tu, J. Brown
Optimizing a remote sensing production efficiency model for macro-scale GPP and yield estimation in agroecosystems
Remote Sensing of Environment, 217 (2018), pp. 258-271
Article Download PDF View Record in Scopus Google Scholar

Massey et al., 2017 R. Massey, T.T. Sankey, R.G. Congalton, K. Yadav, P.S. Thenkabail, M. Ozdogan, A.J. Sánchez Meador
MODIS phenology-derived, multi-year distribution of conterminous U.S. crop types
Remote Sensing of Environment, 198 (2017), pp. 490-503
Article Download PDF View Record in Scopus Google Scholar

Meade et al., 2016 B. Meade, E. Puricelli, W. McBride, C. Valdes, L. Hoffman, L. Foreman, E. Dohlman

Corn and soybean production costs and export competitiveness in Argentina, Brazil, and the United States
EIB-154, U.S. Department of Agriculture, Economic Research Service (2016)
Google Scholar

Monfreda et al., 2008 C. Monfreda, N. Ramankutty, J.A. Foley
Farming the planet: 2. Geographic distribution of crop areas, yields, physiological types, and net primary production in the year 2000
Global Biogeochemical Cycles, 22 (1) (2008), 10.1029/2007GB002947
Google Scholar

Peng et al., 2018 B. Peng, K. Guan, M. Pan, Y. Li
Benefits of Seasonal Climate Prediction and Satellite Data for Forecasting U.S. Maize Yield
Geophysical Research Letters, 45 (2018), pp. 9662-9671
CrossRef View Record in Scopus Google Scholar

Ray et al., 2013 D.K. Ray, N.D. Mueller, P.C. West, J.A. Foley
Yield Trends Are Insufficient to Double Global Crop Production by
Plos One, 8 (2013), p. 2050
Google Scholar

Running et al., 2004 S. Running, R. Nemani, F.A. Heinsch, M. Zhao, M. Reeves, H. Hashimoto
A contiguous satellite-derived measure of global terrestrial primary production
Bioscience, 54 (2004), pp. 547-560
CrossRef View Record in Scopus Google Scholar

Sakamoto et al., 2014 T. Sakamoto, A.A. Gitelson, T.J. Arkebauer
Near real-time prediction of US corn yields based on time-series MODIS data
Remote Sensing of Environment, 147 (2014), pp. 219-231
Article Download PDF View Record in Scopus Google Scholar

Tilman et al., 2011 D. Tilman, C. Balzer, J. Hill, B.L. Befort
Global food demand and the sustainable intensification of agriculture
Proceedings of the National Academy of Sciences of the United States of America, 108 (2011), pp. 20260-20264
CrossRef View Record in Scopus Google Scholar

Trenberth et al., 2013 K.E. Trenberth, A. Dai, G. van der Schrier, P.D. Jones, J. Barichivich, K.R. Briffa, J. Sheffield
Global warming and changes in drought
Nature Climate Change, 4 (2013), pp. 17-22
Google Scholar

USDA, 2018 N. USDA
USDA Crop Production 2014 Summary
US Department of Agriculture (2018)
Google Scholar

Van Niel and McVicar, 2004 T.G. Van Niel, T.R. McVicar
Determining temporal windows for crop discrimination with remote sensing: a case study in south-eastern Australia
Computers and Electronics in Agriculture, 45 (2004), pp. 91-108
Article Download PDF View Record in Scopus Google Scholar

Wagle et al., 2015 P. Wagle, X.M. Xiao, A.E. Suyker
Estimation and analysis of gross primary production of soybean under various management practices and drought conditions
Isprs Journal of Photogrammetry and Remote Sensing, 99 (2015), pp. 70-83
Article Download PDF View Record in Scopus Google Scholar

Wang et al., 2019 S. Wang, G. Azzari, D.B. Lobell
Crop type mapping without field-level labels: Random forest transfer and unsupervised clustering techniques
Remote Sensing of Environment, 222 (2019), pp. 303-317
Article Download PDF View Record in Scopus Google Scholar

Wang et al., 2020 J. Wang, X.M. Xiao, L. Liu, X.C. Wu, Y.W. Qin, J.L. Steiner, J.W. Dong
Mapping sugarcane plantation dynamics in Guangxi, China, by time series Sentinel-1, Sentinel-2 and Landsat images
Remote Sensing of Environment, 247 (2020), p. 111951
Article Download PDF View Record in Scopus Google Scholar

Wardlow and Egbert, 2008 B.D. Wardlow, S.L. Egbert
Large-area crop mapping using time-series MODIS 250 m NDVI data: An assessment for the U.S. Central Great Plains
Remote Sensing of Environment, 112 (2008), pp. 1096-1116
Article Download PDF View Record in Scopus Google Scholar

Wu et al., 2018 X.C. Wu, X.M. Xiao, Y. Zhang, W. He, S. Wolf, J.Q. Chen, M.Z. He, C.M. Gough, Y.W. Qin, Y.L. Zhou, R. Doughty, P.D. Blanken
Spatiotemporal Consistency of Four Gross Primary Production Products and Solar-Induced Chlorophyll Fluorescence in Response to Climate Extremes Across CONUS in 2012
Journal of Geophysical Research-Biogeosciences, 123 (2018), pp. 3140-3161
CrossRef View Record in Scopus Google Scholar

Xiao et al., 2004a X.M. Xiao, D. Hollinger, J. Aber, M. Goltz, E.A. Davidson, Q.Y. Zhang, B. Moore
Satellite-based modeling of gross primary production in an evergreen needleleaf forest
Remote Sensing of Environment, 89 (2004), pp. 519-534
Article Download PDF View Record in Scopus Google Scholar

Xiao et al., 2004b X.M. Xiao, Q.Y. Zhang, B. Braswell, S. Urbanski, S. Boles, S. Wofsy, M. Berrien, D. Ojima
Modeling gross primary production of temperate deciduous broadleaf forest using satellite images and climate data
Remote Sensing of Environment, 91 (2004), pp. 256-270
Article Download PDF View Record in Scopus Google Scholar

Xin et al., 2017 F.F. Xin, X.M. Xiao, B. Zhao, A. Miyata, D. Baldocchi, S. Knox, M. Kang, K.M. Shim, S. Min, B.Q. Chen, X.P. Li, J. Wang, J.W. Dong, C. Biradar
Modeling gross primary production of paddy rice cropland through analyses of data from CO2 eddy flux tower sites and MODIS images
Remote Sensing of Environment, 190 (2017), pp. 42-55
Article Download PDF View Record in Scopus Google Scholar

Xin et al., 2013 Q. Xin, P. Gong, C. Yu, L. Yu, M. Broich, A. Suyker, R. Myneni
A Production Efficiency Model-Based Method for Satellite Estimates of Corn and Soybean Yields in the Midwestern US
Remote Sensing, 5 (2013), pp. 5926-5943
CrossRef View Record in Scopus Google Scholar

Yan et al., 2009 H. Yan, Y.L. Fu, X. Xiao, Q.H. He, H.L. He, L. Ediger
Modeling gross primary productivity for winter wheat–maize double cropping system using MODIS time series and CO2 eddy flux tower data
Agriculture, Ecosystems & Environment, 129 (2009), pp. 391-400
Article Download PDF View Record in Scopus Google Scholar

Yang et al., 2011 C.H. Yang, J.H. Everitt, D. Murden
Evaluating high resolution SPOT 5 satellite imagery for crop identification
Computers and Electronics in Agriculture, 75 (2011), pp. 347-354
Article Download PDF View Record in Scopus Google Scholar

Yuan et al., 2016 W. Yuan, Y. Chen, J. Xia, W. Dong, V. Magliulo, E. Moors, J.E. Olesen, H. Zhang
Estimating crop yield using a satellite-based light use efficiency model
Ecological Indicators, 60 (2016), pp. 702-709
Article Download PDF View Record in Scopus Google Scholar

Yuan et al., 2007 W.P. Yuan, S. Liu, G.S. Zhou, G.Y. Zhou, L.L. Tieszen, D. Baldocchi, C. Bernhofer, H. Gholz, A.H. Goldstein, M.L. Goulden, D.Y. Hollinger, Y. Hu, B.E. Law, P.C. Stoy, T. Vesala, S.C. Wofsy
Deriving a light use efficiency model from eddy covariance flux data for predicting daily gross primary production across biomes
Agricultural and Forest Meteorology, 143 (2007), pp. 189-207
Article Download PDF View Record in Scopus Google Scholar

Zhang et al., 2016 Y. Zhang, X. Xiao, C. Jin, J. Dong, S. Zhou, P. Wagle, J. Joiner, L. Guanter, Y. Zhang, G. Zhang, Y. Qin, J. Wang, B. Moore
Consistency between sun-induced chlorophyll fluorescence and gross primary production of vegetation in North America
Remote Sensing of Environment, 183 (2016), pp. 154-169
Article Download PDF CrossRef View Record in Scopus Google Scholar

Zhang et al., 2017 Y. Zhang, X. Xiao, X. Wu, S. Zhou, G. Zhang, Y. Qin, J. Dong
A global moderate resolution dataset of gross primary production of vegetation for 2000–2016
Scientific Data, 4 (2017), Article 170165
View Record in Scopus Google Scholar

Zhao et al., 2015 Y. Zhao, X.P. Chen, Z.L. Cui, D.B. Lobell
Using satellite remote sensing to understand maize yield gaps in the North China Plain
Field Crops Research, 183 (2015), pp. 31-42
Article Download PDF View Record in Scopus Google Scholar

Zhao and Lobell, 2017 Y. Zhao, D.B. Lobell
Assessing the heterogeneity and persistence of farmers' maize yield performance across the North China Plain
Field Crops Research, 205 (2017), pp. 55-66
Article Download PDF View Record in Scopus Google Scholar

Zhong et al., 2014 L.H. Zhong, P. Gong, G.S. Biging
Efficient corn and soybean mapping with temporal extendability: A multi-year experiment using Landsat imagery
Remote Sensing of Environment, 140 (2014), pp. 1-13
Article Download PDF View Record in Scopus Google Scholar

View Abstract